Conotoxins as Sensors of Local pH and Electrostatic Potential in the Outer Vestibule of the Sodium Channel

Kwokyin Hui,[1] Deane McIntyre,[2] and Robert J. French[1]

[1]Department of Physiology and Biophysics, and [2]Department of Biological Sciences, University of Calgary, Calgary, Alberta, Canada T2N 4N1

ABSTRACT We examined the block of voltage-dependent rat skeletal muscle sodium channels by derivatives of μ-conotoxin GIIIA (μCTX) having either histidine, glutamate, or alanine residues substituted for arginine-13. Toxin binding and dissociation were observed as current fluctuations from single, batrachotoxin-treated sodium channels in planar lipid bilayers. R13X derivatives of μCTX only partially block the single-channel current, enabling us to directly monitor properties of both μCTX-bound and -unbound states under different conditions. The fractional residual current through the bound channel changes with pH according to a single-site titration curve for toxin derivatives R13E and R13H, reflecting the effect of changing the charge on residue 13, in the bound state. Experiments with R13A provided a control reflecting the effects of titration of all residues on toxin and channel other than toxin residue 13. The apparent pKs for the titration of residual conductance are shifted 2–3 pH units positive from the nominal pK values for histidine and glutamate, respectively, and from the values for these specific residues, determined in the toxin molecule in free solution by NMR measurements. Toxin affinity also changes dramatically as a function of pH, almost entirely due to changes in the association rate constant, k_{on}. Interpreted electrostatically, our results suggest that, even in the presence of the bound cationic toxin, the channel vestibule strongly favors cation entry with an equivalent local electrostatic potential more negative than −100 mV at the level of the "outer charged ring" formed by channel residues E403, E758, D1241, and D1532. Association rates are apparently limited at a transition state where the pK of toxin residue 13 is closer to the solution value than in the bound state. The action of these unique peptides can thus be used to sense the local environment in the ligand—receptor complex during individual molecular transitions and defined conformational states.

KEY WORDS: single-channel biophysics • lipid bilayers • peptide toxins • proton block • ion permeation

INTRODUCTION

Under physiological conditions, the degree of protonation of protein side chains plays a key role in determining the catalytic properties of metabolic enzymes, transporters, and ion channels. Among the "P-loop" family of cation channels (e.g., Moczydlowski, 1998), two general kinds of effects of protonation are seen: block of ion conduction through the open channel (or a decrease in maximal conductance in whole-cell recordings) and changes in gating function, with titration of specific side chain carboxylate (Asp, Glu) or imidazole (His) groups being implicated in several cases (De Biasi et al., 1993; Lopes et al., 2000, 2001; Kehl et al., 2002). Changes in pH may also have an important influence on interactions of channels with natural ligands (Vivaudou and Forestier, 1995) or drugs (Hille, 1977a,b; Schwarz et al., 1977; Uehara and Hume, 1985; Zamponi et al., 1993a,b).

In many cases, effects on gating are probably electrostatically induced by titration of fixed charges on the channel protein in the vicinity of the voltage sensor (Frankenhaeuser and Hodgkin, 1957; Hille, 1968; Hille et al., 1975). In some cases, such as the bacterial channel, KcsA, and certain plant channels, protons may play a more direct role in triggering transitions between open and closed conformations of the channel (Heginbotham et al., 1999; Hoth and Hedrich, 1999; Green, 2002).

Although it is now known that the selectivity filter of potassium channels is lined by backbone carboxyl groups (Doyle et al., 1998; Morals-Cabral et al., 2001; Zhou et al., 2001), P-loop residue side chains appear to play a much more direct role in specifying ion conduction and selectivity in voltage-gated Ca and Na channels (Backx et al., 1992; Heinemann et al., 1992; Chen et al., 1996; Sun et al., 1997). For this reason, the detailed effects of protonation might be expected to differ between K channels and Na and Ca channels. The predominant means of inhibition of T-type Ca channels by protonation has been attributed to gating effects (Delisle and Satin, 2000). An earlier, detailed analysis of the effect of protonation on L-type single channel conductance led to the conclusion that the protonation site was separate from the pore but coupled to it by a conformational change (Pietrobon et al., 1989;

Address correspondence to Dr. Robert J. French, Department of Physiology and Biophysics, University of Calgary, Calgary, Alberta, Canada T2N 4N1. Fax: (403) 283-8731; E-mail: french@ucalgary.ca

J. Gen. Physiol. © The Rockefeller University Press • 0022-1295/2003/07/63/17 $8.00
Volume 122 July 2003 63–79
http://www.jgp.org/cgi/doi/10.1085/jgp.200308842

Prod'hom et al., 1989). A later study gave evidence for pH-sensitive transitions between different conductance states resulting from titration of selectivity filter residues (Chen et al., 1996).

In 1968, Hille argued that direct protonation of individual Na channels was responsible for part of the proton-induced block of Na currents (Hille, 1968). Subsequently, a variety of studies have provided evidence for both gating shifts (Hille et al., 1975; Zhang and Siegelbaum, 1991) and direct pore block mechanisms (Woodhull, 1973; Begenisich and Dankó, 1983; Daumas and Andersen, 1993), or a combination of the two (Benitah et al., 1997). Pore block is likely to depend in part on protonation of selectivity filter residues (Sun et al., 1997). A recent analysis, however, shows by mutagenesis that "outer ring" carboxylates, 3–4 residues C-terminal to the selectivity filter, contribute to a complex protonation site (Khan et al., 2002).

In the present work, we make use of pore-blocking μ-conotoxins (Cruz et al., 1985, 1989; Moczydlowski et al., 1986; Lancelin et al., 1991; Sato et al., 1991; Becker et al., 1992) to reversibly introduce a titratable residue into the vestibule of the toxin–channel complex. Derivatives (R13X) of μ-conotoxin GIIIA (μCTX),* in which Arg-13 is substituted by a residue with a side chain that is titrated in a pH range close to physiological pH, provide unique opportunities for observation of effects of protonation in a defined conformational/functional state. We studied the action of R13H and R13E derivatives, using R13A as a control possessing a nontitratable side chain in this position (Fig. 1). Bound times for these peptide toxins are typically ≥1s, which, together with the unique conductance of the bound (partially blocked) state for a given toxin, makes "blocked" and unblocked events easily distinguishable from the channel closed and open times that are limited by channel gating conformational transitions. On yet another time scale, protonation of the channel blocks ion conduction through the pore with rapid kinetics beyond the resolution of our recording system, and is thus seen as a pH-dependent decrease in the amplitude of single-channel current, as in the work of Daumas and Andersen (1993). Thus, although we do not resolve the kinetics of proton block, per se, we were able to continuously monitor the probability of proton block of toxin-bound and -unbound channels. Toxin-binding kinetics depend strongly on pH when a titratable residue is present in position 13. By analyzing the pH dependence, and determining the effective pKs for block of the single channel current, and for toxin binding, we show that the pK of the critical toxin residue 13 is substantially higher than that measured in free solution.

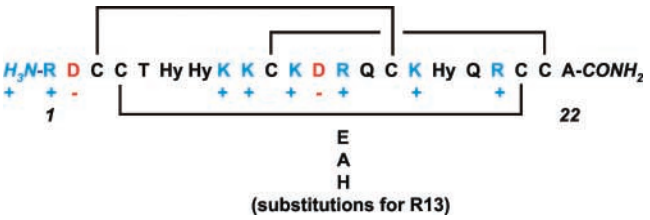

FIGURE 1. Peptide probes based on μCTX GIIIA μCTX GIIIA is a highly basic peptide toxin found in the venom of the fish hunting cone snail, *Conus geographus*. The toxin is held rigidly together by three disulfide bonds and is a potent and specific blocker of skeletal muscle sodium channels. With seven basic and two acidic residues, and an amidated C terminus, this 22-residue toxin has a nominal net charge of +6 at neutral pH. The figure shows its primary sequence, highlighting the charges and disulfide bonds, with basic residues in blue and acidic in red. The N-terminal amine and C-terminal amide groups are shown in italics. In this study, we examined derivatives with three different substitutions for R13: E, A, and H, as indicated on the figure.

We suggest that this shift reflects the ability of the channel vestibule, even in the presence of the bound, cationic toxin, to strongly concentrate protons. We interpret this shift of pKs as a reflection of a substantial electrostatic potential difference between the channel vestibule and the free bathing solution.

MATERIALS AND METHODS

Peptide Synthesis

Peptide synthesis has been described previously (Hui et al., 2002). Briefly, linear peptides were produced by solid phase synthesis using 9-fluorenylmethoxycarbonyl (Fmoc) chemistry. Coupling of Fmoc amino acids was performed using the HBTU/HOBT/DIPEA method on an Applied Biosystems 431A synthesizer. The raw peptides were air oxidized and purified as described previously (Chang et al., 1998). During oxidation, cyclization was monitored by analytical HPLC and usually complete after 2–3 d at 4°C. After folding of the peptide by air oxidation, toxin derivatives were purified to near homogeneity by HPLC (~95%, based on analytical HPLC). Active toxin derivatives were isolated as a single major peak. The identity of purified peptides was confirmed by quantitative amino acid analysis and, in some cases, by electrospray mass spectroscopy molecular weight determination. The proper folding of the toxins was confirmed by 1D and, in some cases, 2D NMR (see RESULTS).

1D and 2D NMR

NMR spectra were recorded at 25°C on a Bruker Avance DMX500 spectrometer operating at a proton frequency of 500.13 MHz and a carbon-13 frequency of 125.76 MHz. All spectra were obtained in aqueous (H_2O or D_2O) solution (450 μL) contained in 5-mm tubes with DSS added as a chemical shift reference. 1D NMR spectra of peptides in H_2O solution (5% D_2O added to provide a lock signal) were recorded using excitation sculpting with pulsed magnetic field gradients (Hwang and Shaka, 1995). The spectra were recorded using the following parameters: 8,000 data points, 128 scans, 6,009-Hz sweepwidth with a 2.68-s recycle time. Spectra were zero killed to 16 K and apodizied using an exponential line-broadening of 0.3 Hz. Proton-detected 2D HMQC

Abbreviations used in this paper: BTX, batrachotoxin; μCTX, μ-conotoxin GIIIA.

spectra were acquired using the following parameters: for the F2 dimension (proton), 2 k data points, 32 scans per increment, sweepwidth 5,482 Hz, recycle time 1.79 s; for the F1 dimension (carbon-13), 320 data points, sweepwidth 25,000 Kz, phase-sensitive spectra (TPPI mode) with GARP decoupling of 13 C during acquisition. Spectra were zero filled to 1 k in the F1 dimension, apodizied with a sine squared window function shifted 72° (F2) and 60° (F1) before transformation.

The high concentrations of toxin required for our experiments (in the μM range) raise the possibility of a nonspecific effect. To ensure that the block was not due to aberrant changes toxin structure, 1D proton NMR was used to check that the folded structures did not deviate qualitatively from that of the wild-type toxin. The proton chemical shifts for the R13X derivatives are generally similar to that of the wild-type toxin, with the exception of the shifts of D12 and Q14, for which some change would be expected in response to substitution at the adjacent position-13. Qualitative NOE data indicates that the basic secondary structure remained the same in all cases tested. Others (Sato et al., 1991; Wakamatsu et al., 1992) have also reported that the R13A and R13K derivatives fold normally.

Vesicle Preparation and Incorporation of Channels into Bilayers

Rat sarcolemmal vesicles were isolated as described in Guo et al. (1987), with some modifications. Muscle tissue was obtained from the fore and hind limbs of adult rats and homogenized in t-tubule buffer (0.1 g/ml sucrose, 2 mg/ml sodium azide, 10 mM MOPS, pH 7.4). Cellular debris and contractile protein were removed by filtering through a gauze pad, low-speed centrifugation and 0.6-M KCl treatment. The membrane-containing fraction was isolated by ultracentrifugation in a 25%/35% (wt/vol) sucrose gradient. The pellet was homogenized in a small volume (<5 mL) of 0.3 M sucrose, 20 mM HEPES solution. The protein concentration (1–3 mg/ml) was determined by the Lawry method using known concentrations of bovine serum albumin for control (absorbance at 595 nm). The preparation was divided into 50 μl aliquots and stored at −80°C. Prior to usage, an aliquot was pretreated with 50 μM batrachotoxin to activate voltage-dependent sodium channels and stored at −20°C (Khodorov, 1985). Generally, the preparation was used 2–30 d after pretreatment.

Channels were incorporated into neutral lipid bilayers (48 μg/μl 1-palmitoyl-2-oleoyl-sn-glycero-3-phosphoethanolamine and 12 μg/μl 1-palmitoyl-2-oleoyl-sn-glycero-3-phosphocholine dissolved in decane) painted onto the aperture, at different initial pH recording conditions. After incorporation, control records were acquired to confirm channel identity and orientation using the single channel conductance, voltage dependence of gating, and sometimes extracellular block by tetrodotoxin. Only single channel incorporations were used in this study. For further details, see the recent paper by Hui et al. (2002).

Bilayer Setup

Experiments were conducted with a bilayer apparatus (Miller, 1986) with an aperture of 90–200-μm diameter separating the two sides. Connection to the patch amplifier was established by 3-M KCl salt bridges filled with a 3% (wt/vol) solution of agar linking the recording chambers to a 3-M KCl sink, in which Ag-AgCl electrodes were submerged. The Ag/AgCl electrodes were connected to an Axopatch-1B amplifier (Bessel filtered at 5kHz, −80 dB), whose output was connected to a Neuro-corder digitizer DR-384. The output from the Neuro-corder was filtered through an 8-pole low-pass Bessel filter (200 Hz, −3 dB), and connected to a Pentium computer (through an Axolab-1 interface, sampled at 1 kHz), a VCR, a Nicolet 2090 digital oscilloscope, and a chart recorder. Data was recorded on the VCR and played back for acquisition to the computer using Fetchex (pClamp 5.5).

Electrophysiology

A solution involving three buffers was used to allow for dynamic changing of the pH. Propionic acid (pK = 4.9; Merck Index Volume 10, pp. 1127) was used as the acidic buffer, MOPS (pK = 7.2) as the neutral buffer, and CHES (pK = 9.3) as the basic buffer. A 200-mM NaCl solution was made using all three of these buffers, at 5-mM concentrations, with 0.1 mM Na_2EDTA. The pH of the recording solution was varied by addition of an appropriate volume of a solution of 200 mM NaOH or HCl dissolved in the same triple buffer as the recording solution. In the case of the HCl solution, at most, 40 μl was used in an experiment resulting in a final [Na] = 195 mM.

Toxin was added to the extracellular side of the channel. Four or more voltages were recorded to determine the single channel current-voltage relationship. Longer records were taken to determine the blocking kinetics. Test voltages generally ranged over ±80 mV; however, more extreme voltages (±105 mV) were sometimes recorded.

Analysis

Current amplitudes and binding kinetics were analyzed in Fetchan and pStat (pClamp 6.0.5). Amplitudes were estimated directly from the current levels within the traces. In most cases this was similar to Gaussian fits of the all-points amplitude histograms; however, we considered it more accurate at and below $V_{1/2}$, when the peaks in histograms became smeared with each other (unpublished data).

Toxin binding events were detected by the half-threshold method in Fetchan (for reviews see Wonderlin et al., 1990; Colquhoun and Sigworth, 1995), setting the levels to the open and blocked states. All events to the open level were included in the detection; however, only events ≥400 ms to the blocked level were included to prevent detection of intrinsic gating closures (Moczydlowski et al., 1984a). With the combined 5-kHz filter from the amplifier, 200 Hz from the 8-pole Bessel filter, and an additional 50-Hz digital Gaussian filter in Fetchan, the dead time for the open events was ~4 ms. The dead time for the block events was the imposed 400 ms. With an average closed time for batrachotoxin (BTX)-activated channels of 22 ms at −110 mV (French et al., 1986), well below 100 ms, this gives a detection of true closures (false positive) at $e^{-400\ ms/100\ ms} < 2\%$. The detection rate of true blocked events, however, varied depending on the block duration. On average, the blocked times were 1 s or longer, giving a detection rate of $e^{-400\ ms/1{,}000\ ms} = 67\%$. So, at worst, one event was missed for every event detected, which would double the estimated open time. To correct for this, the open times were divided by the estimated fraction of detected blocked events (McManus et al., 1987).

Dwell-times were lumped across experiments with same toxin concentration and voltage. The applied voltage was corrected for using the reversal potential offset determined from unblocked channel i-E plots (usually < 10 mV) and rounded to the nearest 10 mV. Since the kinetics of block were only weakly voltage dependent (Fig. 4), the use of a 10-mV bin width does not affect the results significantly. Only histograms with ≥20 events were used in the determination of the time constants. These time constants were corrected for missed blocked events, as described above, before determining the rate constants. The rate constants were taken as:

$$k_{off} = (1/\tau_{blocked}) \quad (1)$$

$$k_{on} = 1/(\tau_{unblocked} \times [Tx]), \quad (2)$$

where $\tau_{blocked}$ is the time constant for the blocked events, $\tau_{unblocked}$ is the time constant for the unblocked ("open") events, and [Tx] is the applied toxin concentration. The dissociation constant, K_d, was independently determined from the block probability:

$$K_d = [Tx] \times (1 - P_b)/P_b = [Tx] \times T_{blocked}/T_{unblocked}, \quad (3)$$

where $T_{unblocked}$ and $T_{blocked}$ are the total times spent in the unblocked and blocked state, respectively, and P_b is the fraction of time the channel is in the blocked state. Because this method does not rely on the presence of a large number of events, K_ds were determined when there were ≥20 (unblocked and blocked) events. The K_d estimated from the ratio k_{off}/k_{on} was generally similar. The voltage dependence of the kinetic parameters was fit to:

$$k = k(0mV)e^{-z\delta FE/RT}, \quad (4)$$

where k is the parameter, k(0 mV) is the parameter at 0 mV, R is the gas constant, F is Faraday's constant, T is the temperature (22°C), E is the applied voltage, and zδ is the apparent valence (a product of the amount of charge, z, and the fractional electrical

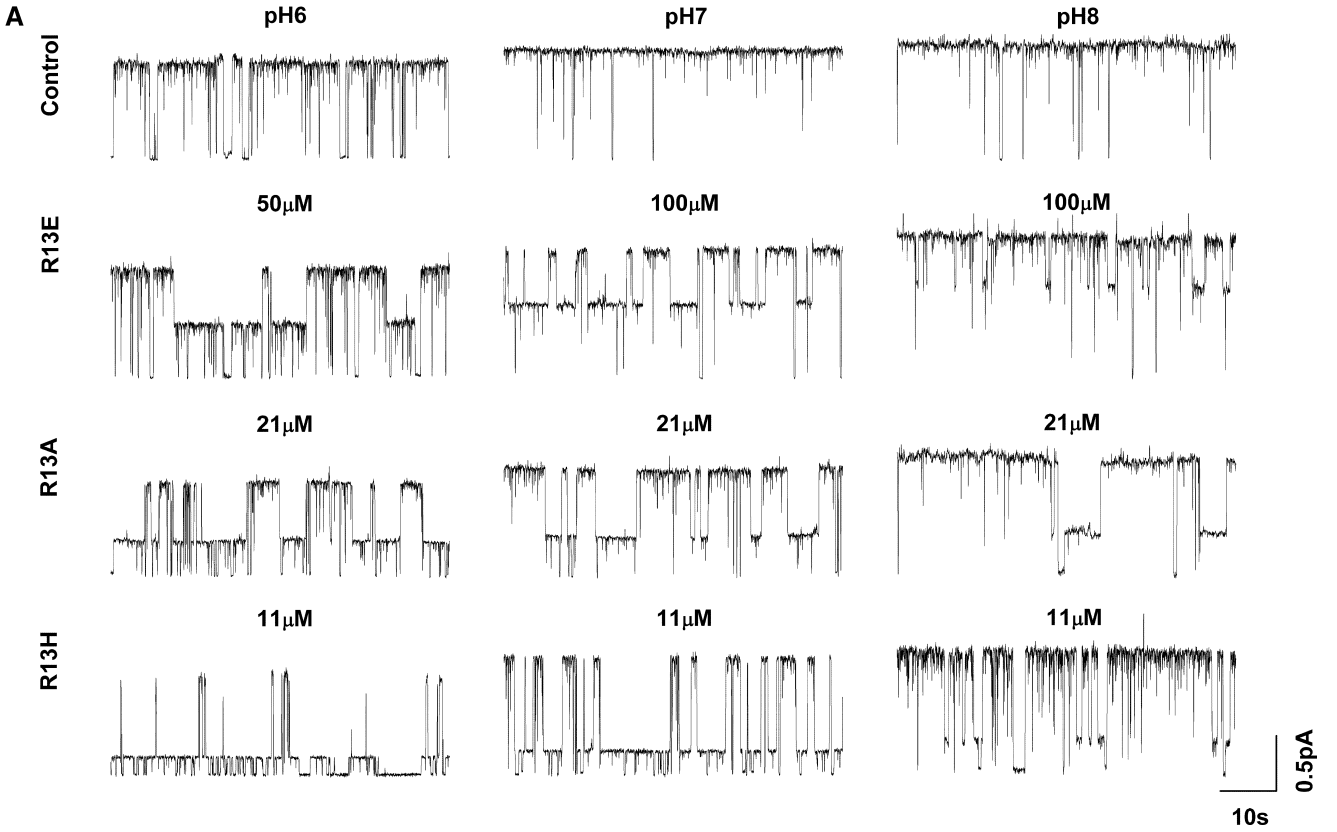

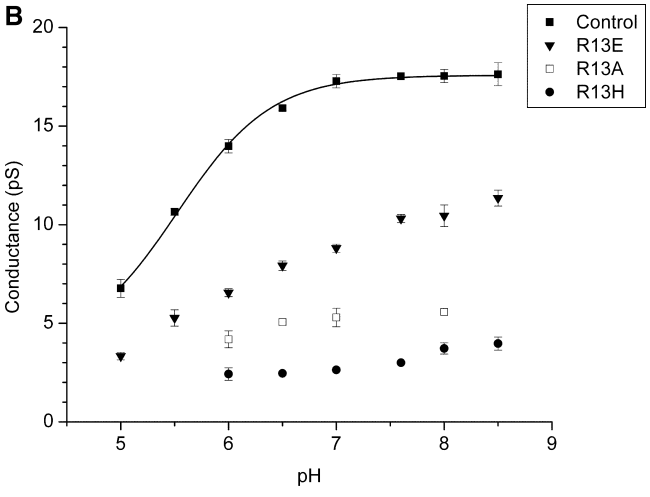

FIGURE 2. Block of single-channel current by μCTX derivatives with titratable or nontitratable residues at position 13. (A) Current traces for R13E, R13A, R13H, and the unblocked (Control) channel at pH 6–8. R13E pH 7.0 and 8 traces are from a single experiment; R13A pH 6.0 and 7 traces are from a single experiment; and R13H traces for all pHs from a single experiment. The control traces represent three different experiments. Concentrations of R13E were 50 μM at pH 6.0 and 100 μM at pH 7.0 and pH 8, with unblocked conductances of 16, 20, and 21 pS, respectively. For R13A, concentration was 21 μM at all pHs (13, 17, and 18 pS for pH 6, 7, and 8, respectively). For R13H, they were 11 μM at all pHs (14, 17, and 18 pS for pH 6, 7, and 8, respectively). Traces shown here were sampled at 1 kHz and digitally filtered (low pass) at 10 Hz. (B) Conductances as a function of pH. Conductance of the unblocked channel, and the residual conductances of the channel bound by either R13E, R13A, or R13H. Conductances were determined from linear fits of current-voltage plots from 3–30 experiments for the unblocked channel, 1–9 for R13E, 1–6 for R13A, and 1–15 for R13H. The unblocked conductance was fit with a single-site titration curve with pK = 5.29 ± 0.03.

distance, δ, through which it moves) (Woodhull, 1973). Values are reported as mean ± SEM.

RESULTS

It is immediately apparent from the single-channel recordings that both the kinetics of μCTX block and the amplitude of single channel currents are strongly dependent on pH (Fig. 2). Toxin binding is visibly favored by acidification, with pH dependence being more dramatic for R13E and R13H than for R13A (Fig. 2 A). This immediately suggests the importance of the residue 13 charge, as titration of channel residues would tend to make the net vestibule charge more positive and therefore generally less favorable for binding of the cationic toxin. Single channel conductance decreases with acidification regardless of whether or not

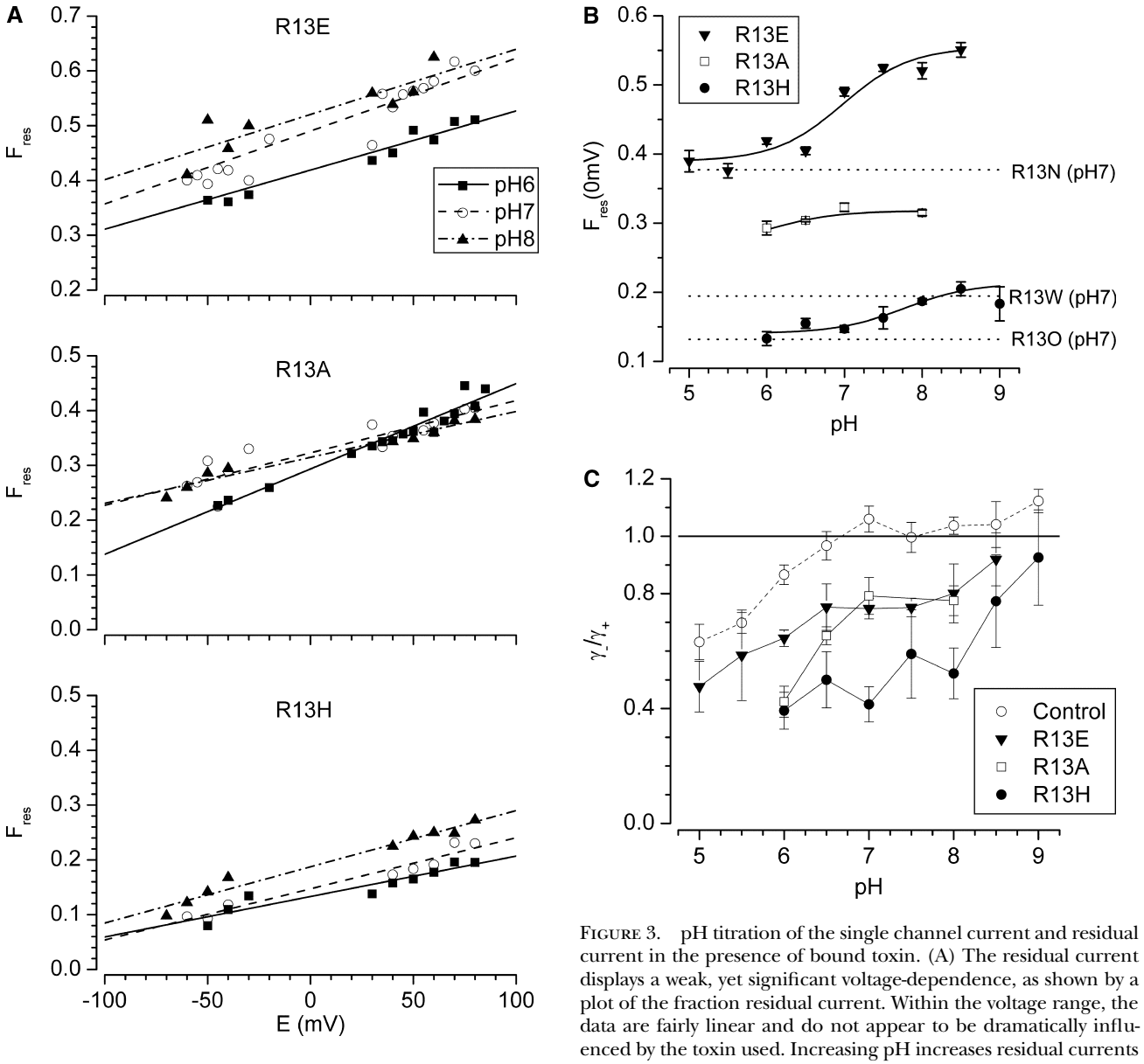

FIGURE 3. pH titration of the single channel current and residual current in the presence of bound toxin. (A) The residual current displays a weak, yet significant voltage-dependence, as shown by a plot of the fraction residual current. Within the voltage range, the data are fairly linear and do not appear to be dramatically influenced by the toxin used. Increasing pH increases residual currents with both R13E and R13H, but has no significant effect for R13A. F_{res}(0 mV) was defined as the fraction residual current at 0 mV determined from the linear fits. This parameter was used to compare the block for different toxin-pH combinations. (B) F_{res}(0 mV) follow simple titration curves only for R13E and R13H. In contrast, the residual current for R13A is nearly constant down to pH 6, below which it may decrease slightly (an arbitrary smooth curve is drawn through the R13A data points). For comparison, F_{res}(0 mV) for R13N, R13W, and R13O at pH 7.0 are shown (from Hui et al., 2002). Data for each point were lumped from 1 to 15 experiments for each toxin. (C) The rectification of the control and residual single channel currents is weakly dependent on pH. The ratio of the residual conductances at negative and positive voltages clearly shows the outward rectification property of the toxin-bound channels. (Any value of the conductance ratio $\neq 1$ reflects a nonlinear single-channel i-E relation; values <1 reflect accentuated proton block at negative voltages.) This behavior is also exhibited by the unblocked channel for pH < 6, as reported previously by Daumas and Andersen (1993). The rectification is strongest at low pH, and diminishes as pH increases.

the channel is bound—and partially blocked—by toxin (Fig. 2 B). The apparent pK for titration of the single channel conductance (5.29 ± 0.03) is close to the value of 5.5 determined for proton block of ^{22}Na influx through BTX-modified channels in two different cell lines (Huang et al., 1979). Daumas and Andersen (1993) reported a single-site apparent pK of ~4.9 in symmetric 1 M NaCl, in a bilayer study of BTX-activated rat brain Na channels. Recent estimates for cloned skeletal muscle channels ($Na_v1.4$) expressed in amphibian oocytes or mammalian cells, made in the absence of BTX, tend to cluster in the range of 5.9–6.1 (Benitah et al., 1997; Sun et al., 1997; Khan et al., 2002). We speculate that small shifts in pK may arise both from BTX modification and from changes in ionic strength (see also the section below on NMR measurements of side chain pKs in conotoxin derivatives).

Titration of Residue 13 Modulates the Fractional Block of Single Channel Current

We showed previously that R13X derivatives of μCTX induce discreet, partial block of the unitary current through sodium channels (Becker et al., 1992) and that the fractional block of current is linearly dependent on the charge on residue 13 (Hui et al., 2002). Superposed on the effect of residue 13 charge, a steric contribution was identified. We examined here the residual current for derivatives with titratable substitutions, glutamate and histidine, using alanine as a control with a nontitratable side chain. This allowed us to reexamine the effect of changing the charge with minimal size change. Consistent with our previous study, at pH 7, R13H (basic) blocked most effectively, followed by R13A (neutral) and then R13E (acidic; Fig. 2 A). To focus on the effect of titration of the toxin, we examined the dependence of $F_{res}(0)$, the fractional residual current when the toxin is bound to the channel, on pH (Fig. 3, A and B). $F_{res}(0)$ changes after a single site titration curve for R13E and R13H, with little change as pH varies for R13A. These R13A data suggest that, in the range examined, there is no substantial titration of any residue important to determining $F_{res}(0)$ other than toxin residue 13. Thus, we interpret the data in Fig. 3 B as a direct reflection of the effect of titrating residue 13 on the fractional residual current. Apparent pKs for titration of R13E (7.0 ± 0.1) and R13H (7.8 ± 0.3) are shifted 2–3 pH units positive from "typical" values shown by these side chains in proteins (Table I), suggesting a higher proton activity in the vestibule than in free solution.

A practical limitation in these experiments arises from the proton-induced block and gating shifts. The voltage dependence of gating, as estimated from $V_{1/2}$, is also shifted to as high as approximately −40 mV at pH 5. These two effects reduced our ability to resolve the amplitude of single channel fluctuations, especially at negative potentials, with the small residual currents for the toxin derivatives R13H and R13A, so in these cases residual current data were used only down to pH 6. However, discrete binding events for these two toxins were identifiable by eye and were examined down to pH 5.5.

Proton Access to the Pore Is Only Weakly Impeded by Bound Toxin

With R13A or other derivatives bound, reduction in residual current after acidification was apparent, indicating that protons continue to have ready access to the vestibule (Fig. 2 B). However, reduction of the R13A residual conductance went roughly in parallel with proton block of unbound channels, resulting in the observed minimal dependence on pH of $F_{res}(0)$ for R13A (Fig. 3 B). Moreover, the residual current for R13E and R13H was noticeably smaller at low compared with high pH, indicating that at least residue 13 was being titrated. Since low pH is expected to favor the protonated form of the substituted residue, these results provide rigorous confirmation of the residue 13 charge dependence of current block by μCTX.

The presence of these highly charged, partially blocking toxins in the vestibule was shown previously to induce weak rectification of residual current (see also Fig. 3 A), presumably resulting from an asymmetric electrostatic barrier to sodium permeation (Hui et al., 2002). To determine if proton accessibility was likewise impeded, we examined whether rectification of the residual current was pH dependent.

Fig. 3 A shows that the residual current is generally slightly larger at 40 mV than at −40 mV. This trend is slightly pH dependent, with higher pH reducing the difference. Fig. 3 C presents the rectification explicitly as the ratio of conductance determined at negative and at positive voltages, thus showing that there is a component of rectification associated with acidification in

TABLE I

Summary of Titrations—Apparent pKs of Toxin Residues and of Block

Residue substituted for R13	Nominal[a]	NMR (free toxin in solution)	F_{res} (bound toxin)	Kinetics (K_d, k_{on})
Glu	4.3–4.5	3.85 ± 0.04	7.0 ± 0.1	probably ~6–7
His	6.0–7.0	5.65 ± 0.02	7.8 ± 0.3	6.4 ± 0.1, 6.4 ± 0.1[b]

[a]From Table 1.2 of Creighton (1993). Ranges taken from various model compounds. Sidechain pKs for free amino acids are 4.1 (Glu) and 6.0 for His.
[b]Approximate pKs from K_d and k_{on}, respectively, from the limited dataset (Fig. 6).

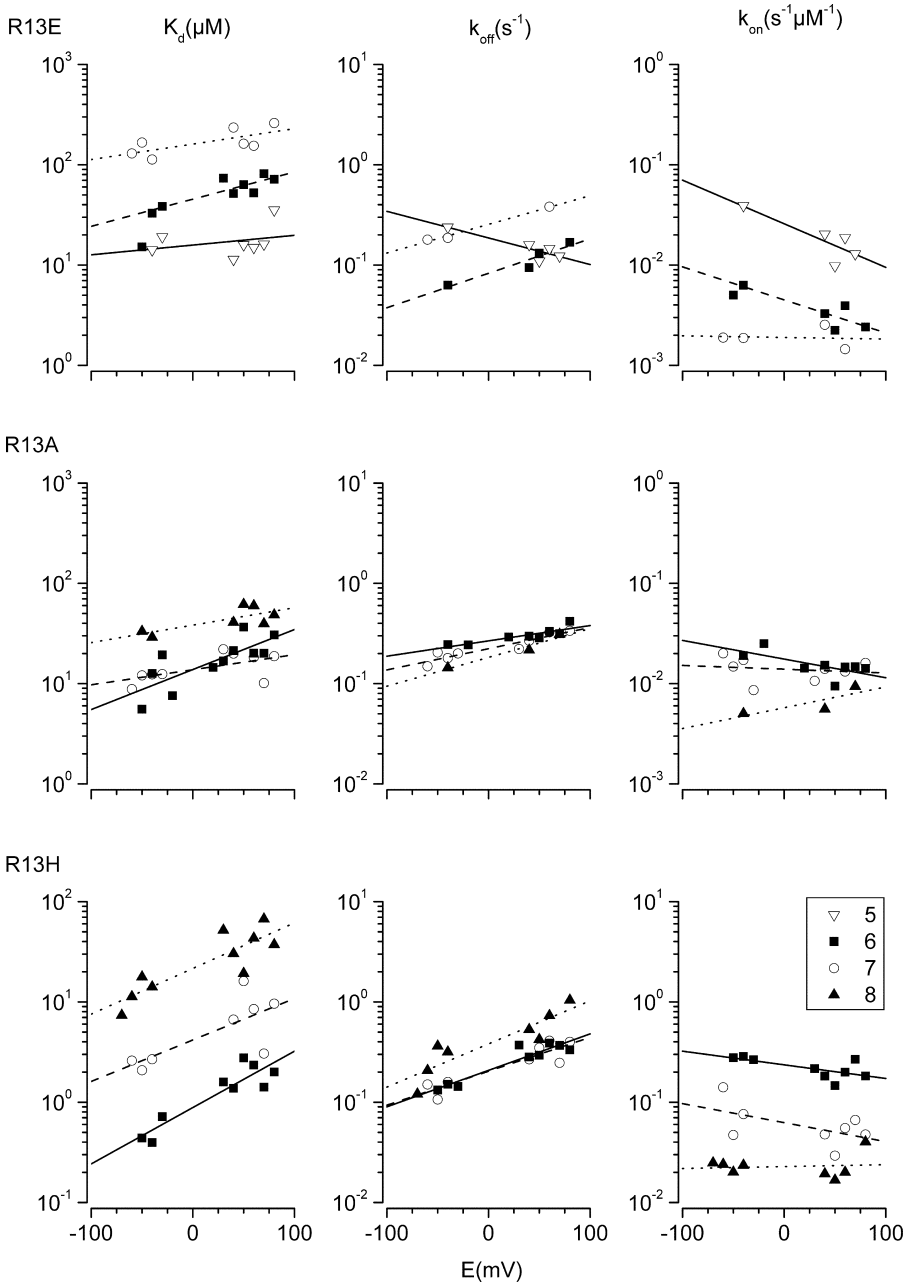

FIGURE 4. Voltage and pH dependence of toxin binding. μCTX derivatives show weakly voltage-dependent block, consistent with their binding at a relatively superficial site in the vestibule. Although there is some dependence on the identity of the residue 13 substitution, the effective valence (zδ) is not significantly altered by pH. Each data point reflects the exponential fit of a dwell-time histogram with ≥20 events (average = 83). The lines represent linear fits on the semilog plots, from which the values at 0 mV are used for comparison of the different toxin-pH combinations. The k_{off} fit for R13E at pH 5.0 appears to have a negative voltage dependence, which is probably artifactual, because the single point at −40 mV was estimated from a total of only n = 21 events and other points are too tightly clustered on the abscissa to strongly influence the slope. The dissociation constant, K_d, and the rate constants (k_{off} and k_{on}) are shown for R13E, R13A, and R13H. The key observation is that the K_ds and k_{on}s for R13E and R13H consistently show a monotonic dependence on pH (see data in the four corner panels of the figure).

both toxin-bound and -unbound channels. The fact that the rectification ratio is decreased over the whole pH range confirms that the toxin binding, per se, induces some rectification. The differing ranges over which rectification changes with pH for the different derivatives reaffirms that the effective pK for the titration of the conductance depends on the identity of the residue that has been introduced into the vestibule by toxin binding, with histidine facilitating proton block over alanine and glutamate. Clearly, however, protons have free access to the vestibule regardless of the chemical identity of residue 13, despite the fact that the different substituents, glutamate, alanine, and histidine differ substantially in their efficacy at blocking Na current through the channel. This allows us to use these titratable substituents as direct measures of the effective local pH, and by inference, local electrostatic potential.

The fact that the presence of bound toxin does not preclude or severely inhibit free access of protons to the pore may seem counterintuitive, but it is not surprising in the light of the substantial residual current carried by Na^+ in the presence of the toxin derivatives. It could reflect in part the finite range of electrostatic effects of the toxin charges—an intravestibular space constant for electrostatic effects was previously estimated at ~8 Å (Hui et al., 2002). This is consistent with the small effects of other toxin charges on the residue 13 titration detected in the NMR measurements (see

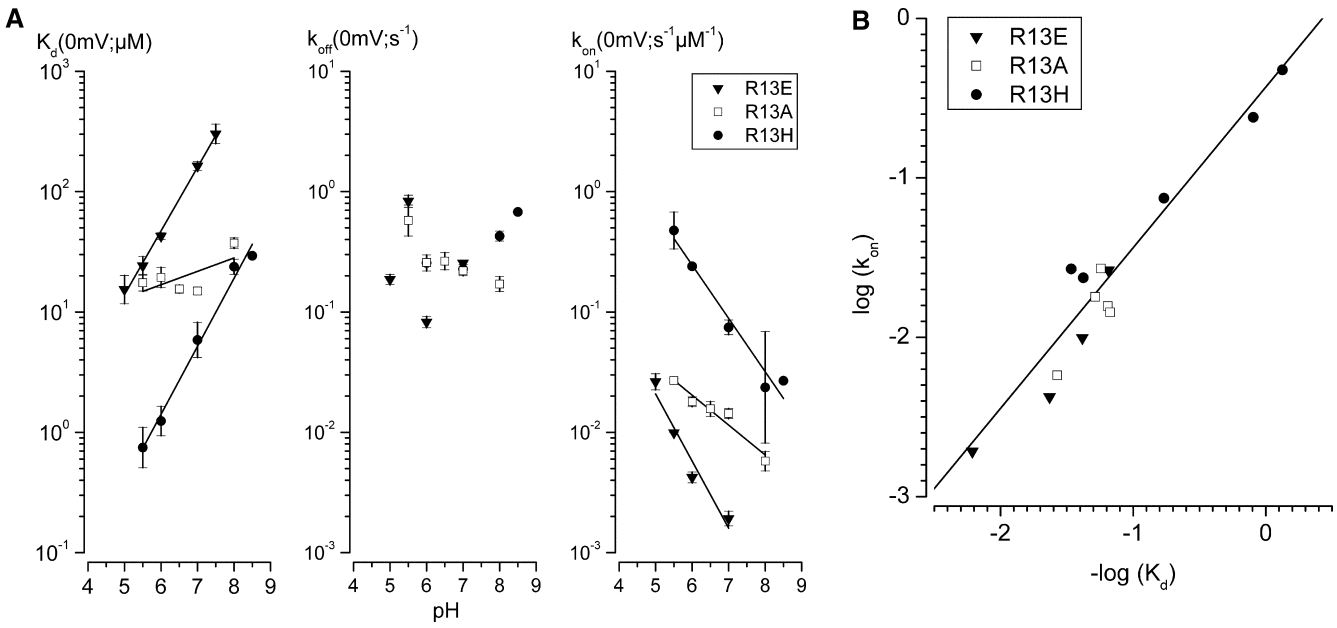

FIGURE 5. The pH dependence of the association rate constant determines the pH dependence of toxin binding. (A) The K_d of block is pH dependent, and is more strongly so for the titratable toxins, R13E and R13H. This is consistent with an electrostatic component in toxin block contributed by residue 13. With a nontitratable A13 side chain, R13A shows little or no pH dependence. The effect of pH on K_d resides in the on rate and not off rate, with a clear correlation between higher pHs and slower binding rates. It is noteworthy that k_{on} for R13A appears to show a similar, but distinctly weaker, trend, probably arising from the combined titration of pore carboxylate residues and D2 and D12 on the toxin. In contrast, k_{off} does not display a clear dependence on pH. (B) The combined data for all three derivatives shows a high correlation between log k_{on} and $-\log K_d$ in a Brønsted plot (slope 1.0 ± 0.1).

below), and also with the possibility that there may be alternate pathways for protons to enter the channel (see final section of DISCUSSION). An alternative scenario has been proposed to account for the independent titration of two neighboring acidic sites in the pore of a cyclic nucleotide–gated channel (Root and MacKinnon, 1994) in which charged sites are associated with counter ions most of the time, and thus do not interact electrostatically.

pH Dependence of Toxin Binding Affinity

High affinity pore block of cation channels generally appears to depend on positive charges on the blocker. In the case of charybdotoxin and related toxins blocking potassium channels, the on rate is reduced by neutralizations of certain residues (Stocker and Miller, 1994). Moreover, a protruding lysine residue is known to compete with potassium binding at an external site in the permeation pathway. Neutralization of this residue severely disrupts binding. This lysine is analogous to arginine-13 in μCTX. From the single-channel traces we see that the kinetics of toxin binding is clearly dependent on residue 13 charge (Fig. 2). The weakest block was observed for R13E, with K_d in the order of tens of μM at pH 7. R13H was ~10-fold more potent, with R13A in between the two. So, although arginine-13 is important for μCTX binding, its neutral substitution does not completely disrupt the interaction (Sato et al., 1991; Becker et al., 1992; French and Dudley, 1999).

In this study, we directly examined the importance of residue 13 charge by titration of R13E and R13H. Lowering the pH strongly enhances binding by the R13E and R13H, but only relatively weakly affects the binding of R13A, consistent with the major contribution of residue 13 to high affinity binding (Figs. 2, 4, and 5). The voltage-dependence of the equilibrium dissociation constant was not systematically pH dependent (Fig. 4) and is similar to that reported for wild-type toxin (unpublished data; Cruz et al., 1985; Becker et al., 1992), further indicating that the mutations did not cause dramatic changes in toxin-channel structure.

We plot the parameters determined at E = 0 mV—the preexponential component of Eq. 4—against pH to ascertain how the titration of the toxins affects affinity and the kinetics of binding (Fig. 5 A). In the case of R13E and R13H, a 2 U increase in pH results in a >10-fold increase in K_d. This is not surprising, since the high pH lowers residue 13 charge, which has a direct impact on affinity. The K_d values increase exponentially with pH and do not saturate within the range examined. Interestingly, the change in affinity can be explained almost completely by the variation of the association rate, which also shows a simple exponential dependence on pH. The dominant role of the association

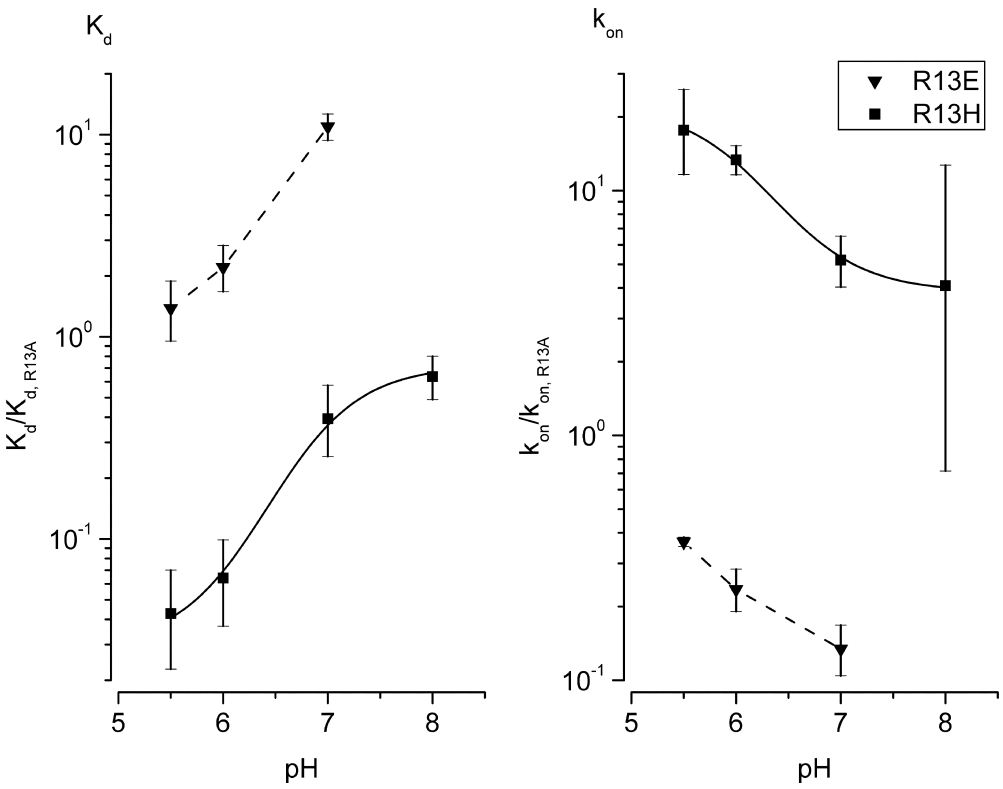

FIGURE 6. Effect of residue 13 titration on binding kinetics. The isolated effects of residue 13 in R13E and R13H are estimated by normalizing parameters against the corresponding values for the "non-titratable" R13A derivative. Although this reduced the range over which we could determine reliable estimates, the normalized K_d and k_{on} for R13H both appear to follow titration curves with pKs of 6.4 ± 0.1. Residue 13 in R13E also appears to be titrated, but does not saturate within the range of the data. Lacking an obvious tendency toward plateau values, we did not attempt to fit the R13E data (dotted lines simply connect the data points).

rate constant in determining the pH dependence is emphasized in Fig. 5 B, where the combined data for all three derivatives are superposed in a Brønsted plot. The correlation between binding and pH suggests that the association rate is dominated by simple electrostatic forces. In contrast, when all the derivatives were considered collectively, there was no obvious trend shown by the dissociation rate constant, which is consistent with the idea that short range forces determine dwell times for the toxin bound to the channel.

Somewhat unexpectedly, R13A kinetics showed a similar pH dependence (see Fig. 5 B), albeit much weaker than for the other two toxin derivatives. Although the equilibrium dissociation constant did not significantly change, the on and off rates both appear to decrease with pH. These changes reflect the net result of titration of any pH-sensitive groups on either channel or toxin, other than the residue 13 side chain. The equilibrium dissociation constant for R13A shows no convincing trend with pH changes, but this, in fact, reflects approximately parallel decreases in k_{on} and k_{off} with increasing pH. Simplistically, this would be consistent with k_{on} being dominated by protonation of toxin residues (favoring association), and k_{off} being dominated by protonation of the channel (favoring dissociation). This might arise if the two rate constants were limited at different points along the reaction coordinate, consistent with, but not demanding, the notion that the association rate constant is controlled primarily by long-range interactions, whereas the dissociation rate constant is limited by short range interactions.

To resolve the complication that multiple charges influence binding kinetics, we normalized the kinetic parameters from R13E and R13H with respect to R13A. Assuming that the effects of residue 13 are independent of those responsible for changes in R13A binding, this normalization isolates the effects of residue 13. In support of that assumption, the normalization results in an R13H dose–response curve that appears to saturate in a manner consistent with a single site titration, contrasting nonnormalized results (compare Figs. 5 and 6). Moreover, the approximate pK for R13H binding (pK = 6.4 ± 0.1) is between free solution values determined by NMR and that for titration of the bound state represented by $F_{res}(0)$ (see following section and Table I). This supports the hypothesis that the R13H starts in bulk solution with an apparent pK of ~6 for His-13 and moves progressively into a proton-enriched environment as it approaches its receptor, where, in the bound state, the apparent pK is ~8.

μCTX Residue 13 as a pH Sensor—Calibration by NMR Determinations of pK for E13 and H13

Although the nominal pK for histidine and glutamate range from ~6–7 and 4.3–4.5, respectively (Creighton, 1993), within the toxin derivatives they are likely different because of the abundance of basic side chains on the toxin. The pKs for the histidine and the glutamate

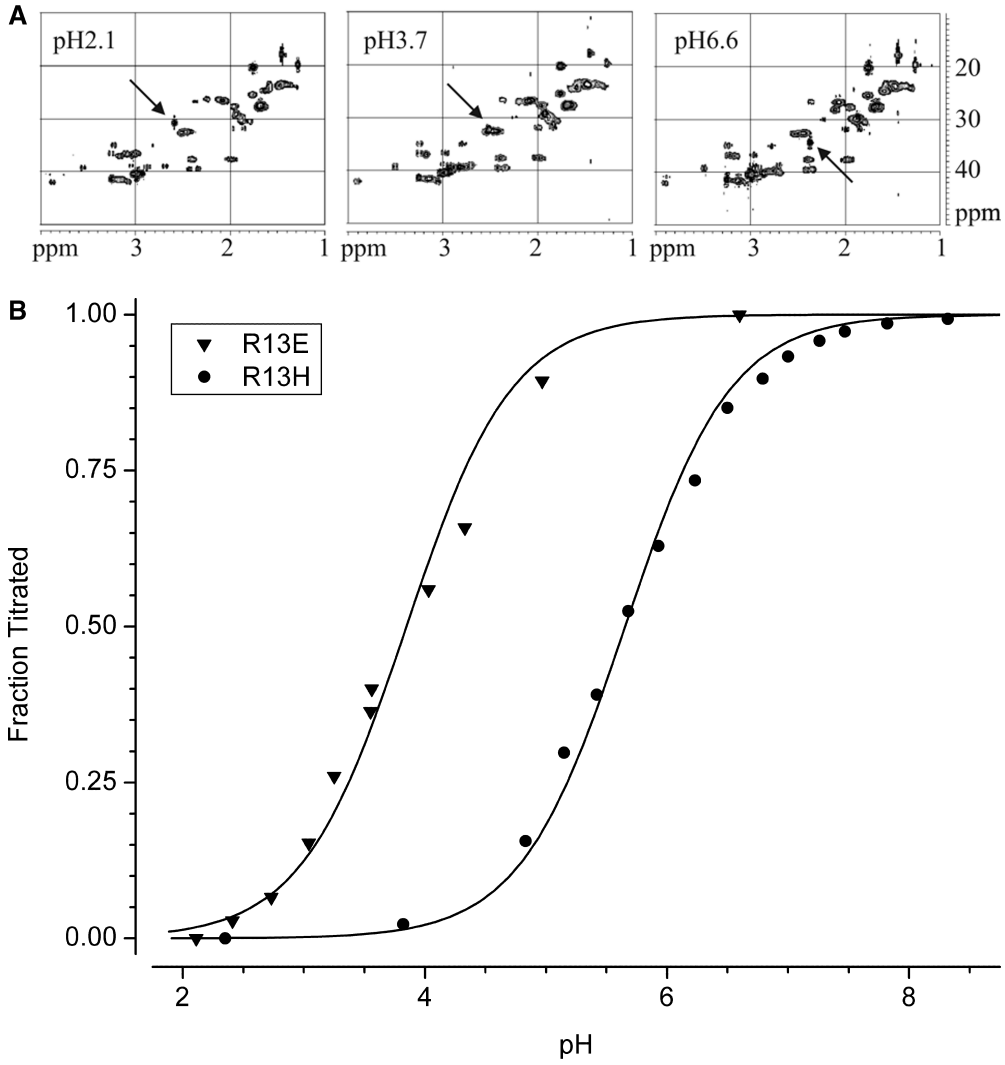

FIGURE 7. pKs of residue 13 for μCTX derivatives measured in free solution. (A) Two-dimensional NMR of the titration of R13E. The arrow shows the carbon-13 shift of the E13 gamma carbon, which was followed during the course of the titration between pH 2.1 to 6.6. *B.* The titration of residue 13 is shown here for R13E and R13H, determined from their NMR spectra, indicating nominal (solution) pKs of 3.85 ± 0.04 and 5.65 ± 0.02, respectively. For comparison, the titration curve of the unblocked channel is found between them with a pK of 5.29 ± 0.03 (see Fig. 2 B).

in the R13H and R13E mutants, respectively, were determined by recording 1D proton NMR spectra in D_2O solution at various pH values. The pH was measured using a Corning pH meter, model 140, equipped with an Orion mini pH electrode that could be inserted directly into the NMR sample tube. The pH of the samples was adjusted by microliter additions of 0.1 M solutions of DCl or KOD (D = ^{2}H). After measurement of the pH, spectra were recorded with presaturation of the residual water. The chemical shifts, referenced to DSS (0 ppm), were measured for the His 2H and 4H protons for the R13H mutant and for the glutamate gamma protons for the R13E mutant. In the latter case, overlap with other signals was observed at some pH values but it was still possible to measure the chemical shift with reasonable precision. In the case of the R13E mutant, the carbon-13 shift of the glutamate gamma carbon was also determined from proton-detected 2D HMQC spectra (Fig. 7 A). Carbon chemical shifts were referenced to DSS (−1.6 ppm). The pK was determined in each case by a single site dose response curve fit of the observed chemical shifts as a function of pH (Fig. 7 B). The pKs of both residues determined in this manner were 3.85 ± 0.04 for E13 and 5.65 ± 0.02 for H13, at least two units lower than estimates from the residual current (6.98 and 7.85, respectively). Moreover, the apparent titration range of these two residues flanks that for titration of the channel conductance (pK = ∼5.29 ± 0.03; Fig. 2 B).

When the pKs were remeasured in the presence of 200 mM NaCl, they were each shifted by about 0.35 pH units. This indicates that there is relatively little influence on the residue 13 pK from the other charges on the toxin, but that protonation is favored slightly by screening the additional positive side chains of the toxin at higher salt. The single channel conductance titration curve (Fig. 2 A) may reflect an analogous small shift toward lower pH compared with values that would have been obtained in the lower ionic strength solutions used in oocyte and mammalian cell studies. However, these shifts are small compared with the differences between the NMR-determined pKs and the

values determined from the single channel measurements. Thus, it appears that the pKs for titration of F_{res} (Fig. 3 B) and the normalized binding kinetics (Fig. 6) are largely determined by local conditions in the vestibule of the channel.

DISCUSSION

Overview

The major experimental findings of this study are that: (a) Increasing the charge on μCTX residue 13 by protonation increases the toxin's fractional block of the single Na channel current. (b) Proton block of unitary current occurs readily, though with measurably different characteristics, in both toxin-bound and unbound channels. (c) Protonation of residue 13 increases binding affinity by increasing the association rate constant. (d) Effective pKs for titration of kinetic parameters (equilibrium K_d and association rate constant, k_{on}) and the residual current shifted positively from the pK for titration of residue 13 in free solution. We believe that the simplest interpretation of these results is that protons are electrostatically concentrated in the vestibule, even in the presence of the bound toxin, and that a titratable residue at position 13 of the toxin provides a molecular-scale sensor of local pH in the vestibule.

Separating the Contributions of Charge and Size to Single-channel Block

Previously, we reported that the residual current in μCTX-bound sodium channels was directly affected by the charge of toxin residue 13 (Hui et al., 2002). In that study, different amino acid substitutions were made of toxin residue 13, so we could not definitively isolate the electrostatic and steric contributions to current block. Moreover, we also found a significant, secondary effect of residue 13 size on the residual current. Consistent with our previous study, the residual current of μCTX blocked channels is dependent on the charge of toxin residue 13 for the titratable derivatives. In addition, the pH dependence of the residual current (for R13E and R13H) is consistent with the titration of a single site, likely residue 13.

In the previous study, $F_{res}(0)$ for the residue 13 μCTX derivatives was shown to depend most dramatically on the charge of residue 13 (0.199 ± 0.002 per unitary charge), and secondarily on side chain size (length dependence, 0.060 ± 0.007 per Å, in a range of ~4–8 Å). Since protonated and unprotonated forms of titratable residues, glutamate and histidine, differ by a single proton (~1.1 Å) that is delocalized over the functional group, the size contribution to any changes in current block would be $<0.06 \times 1.1 = 0.066$. Hence, any change in fractional block >0.066 is probably due to a charge change of residue 13. With R13E, pH titration of the residual current resulted in a 0.17 change in F_{res}, indicating a charge change in residue 13. Moreover, in its "protonated" form, R13E resembles R13N in its degree of current block. With R13H, however, pH titration of the residual current results in a 0.07 change in F_{res}. Although this might plausibly be explained solely by steric effects, there are three reasons to suggest otherwise. First, the pH dependence conforms to a single site titration, consistent with the involvement of only a single residue. Second, the pH range tested covers that of the pK of histidine reported in free solution and other proteins. Third, the titration profile saturates at both ends within the test range, which (in conjunction with the second point) suggests that a histidine was titrated during the experiments.

Thus, we conclude that the change in current block by R13E and R13H resides mostly in electrostatic contributions from residue 13. The pKs of these residues estimated from the titration of F_{res} are 7.0 ± 0.1 and 7.8 ± 0.3, respectively. These values exceed the NMR determinations of pK for these residues by 3.15 and 2.15 pH units, respectively. Apparently, the effective pKs of residue 13 in R13E and R13H are different when the toxin is bound to the channel from their values in free solution. A simple rationale for this observation is that the local pH within the toxin-bound pore is different from that in free solution.

Electrostatic Concentration of Protons in the Channel Vestibule

It is not surprising that the pH in a cation-selective channel vestibule might be lower than in the bathing solution. Although the lipid used in our system may be "neutral," the high degree of glycosylation, and the presence of pore-lining side-chain carboxylates in the channel, contribute to a negative surface potential that would locally concentrate cations. The presence of a bound, positively charged μCTX molecule in the pore would be expected to moderate this local concentration of cations, contributing to a reduction in the unitary current. With our μCTX residue 13 derivatives, we attempted to measure the local electrostatic effect by estimating the local proton concentration in the toxin-bound vestibule of the channel, based on the titration of the fractional residual current. To simplify the comparison of different toxin variants, we used the fractional residual current, interpolated to 0 mV (Hui et al., 2002) as a standard measure of the single channel current in the toxin-bound state.

$F_{res}(0\ mV)$ appears to follow a single site titration for R13E and R13H, while there was no significant pH dependence for R13A ($P = 0.27$; Fig. 3 B). For R13E, $F_{res}(0\ mV)$ titrated with pK = 6.98 ± 0.09, showing upper and lower bounds of 0.390 ± 0.006 and 0.555 ± 0.008, respectively. This indicates that the protonated form of R13E functionally resembles R13N at neutral

pH, with an $F_{res}(0\ mV) = 0.38$, which is consistent with the van der Waal's volumes for the glutamate (109 Å^3) and asparagine (96 Å^3). For R13H, titration proceeded with a pK = 7.85 ± 0.36, bounded at 0.141 ± 0.006 and 0.22 ± 0.02 on the lower and upper ends, respectively. In this case, the protonated form of R13H yields a residual current similar to R13O ($F_{res}(0\ mV) = 0.13$), also consistent with the similar van der Waal's volumes for histidine (118 Å^3) and ornithine (117 Å^3). The neutral form, however, appears to resemble R13W ($F_{res}(0\ mV) = 0.19$; 163Å^3), perhaps indicating some special role of the ring structures in steric block.

Since protons continue to have access to the pore of the toxin–channel complex, and since the fractional residual current for R13A was not significantly changed by pH, Fig. 3 B allows an estimate of the effective pK of residue 13 for R13E and R13H. These estimates, ~7 for E13 and ~8 for H13, are higher than values commonly observed in proteins (4.3–4.5 for glutamate and 6–7 for histidine; Creighton, 1993), as well as our own NMR determinations. If the chemical properties of the side chains are unchanged, the data would be consistent with local pH > 2 pH units lower than bath pH.

Estimating the Local Electrostatic Potential in the Channel Vestibule

Protons induce a fast block of the sodium channel that is observed as an apparent reduction in the single channel current (Benitah et al., 1997). The wild-type sodium channel is blocked by protons with an apparent pK between 4 and 5 (Woodhull, 1973), and only ~0.5 U higher for batrachotoxin-activated channels (Huang et al., 1979). Although a complete titration curve of the sodium channel activity was not attempted in this study, our data are sufficient to estimate a pK of 5.29 ± 0.03 (Fig. 2 B), which compares favorably with the previous determinations.

A noteworthy finding in our present study is that although the μCTX derivatives partially occlude Na ions from permeating through pore, they do not prevent protons from blocking the channel. This is demonstrated by the lack of pH apparent dependence of F_{res} for R13A, indicating that the channel is being titrated normally even with the toxin bound to it. Since toxin residue 13 binds closest to the selectivity filter, it should sense the local pH within the pore's vestibule. On this basis, we estimated the pH difference between bath and vestibule solution by comparing the pK of the titratable toxins (R13E and R13H) in free solution and channel-bound configurations. The results indicate that the pH at the channel vestibule is at least 2 U lower than in bulk solution, which is also supported by the pH dependence of the kinetics. This means that, when referenced to local pH rather than the value in solution, the proton block site on sodium channels may actually have a pKof ~5.3 − 2 = 3.3, a value more typical of a carboxylate group.

The proton concentration difference between pore and free solution can be used to estimate the potential within the pore. The difference between the two concentrations can be described by the Boltzmann equation:

$$[H]_p = [H]_\infty \exp(-z_H \psi F/RT), \quad (5)$$

where $[H]_p$ is the proton concentration within the pore, $[H]_\infty$ is the concentration in free solution, $z_H = +1$ is the charge of a proton, ψ is the local potential in the channel pore, and RT/F = 25.3 mV at 20°C. Eq. 5 simplifies to:

$$\psi = -(\Delta pH \times RT/F)/(0.434 z_H), \quad (6)$$

so that the local potential can be estimated directly from the difference in pH between pore and free solution (ΔpH). We define ψ as an equilibrium parameter at the pK of the group being titrated; in general, its value will depend on the whole electrostatic environment, including the complete array of toxin and channel charges in the neighborhood. It should be noted that any conformational changes, changes in charge, or shifts in position of different charged groups could affect the estimated value of ψ. With ΔpK ~2, the local potential is approximately −117 mV, favoring concentration of cations in and near the vestibule. This is a surprisingly large value, especially given the presence of the toxin, and is approximately twice the magnitude estimated in two different studies (Green et al., 1987; Khan et al., 2002). Despite the care and attention to detail in these analyses, there are several possible reasons for the quantitative discrepancies. Green et al. (1987) used an analysis of conductance-concentration relations with TEA and Ba^{2+} as ion substitutes to maintain ionic strength to estimate the surface potential near the pore mouth. A later study (Naranjo and Latorre, 1993) concluded that estimates of surface charge (and hence, potential) by this general approach are quite sensitive to the choice of ionic conditions. A further complication is that the particular model for ion permeation, to which the calculation of surface potential is coupled, also influences the quantitative outcome. In the study by Khan et al. (2002), the estimate of local potential near vestibular protonation sites of −58mV, was clearly identified as a conservative lower limit. This was based on their experimental estimates of the change in pK for titration of channel conductance per unit charge change introduced by point mutations in the "outer charged ring" of the pore. If one uses their upper limit of ΔpK = 0.4 per unit charge, rather than the lower limit of 0.25, then the estimated potential near

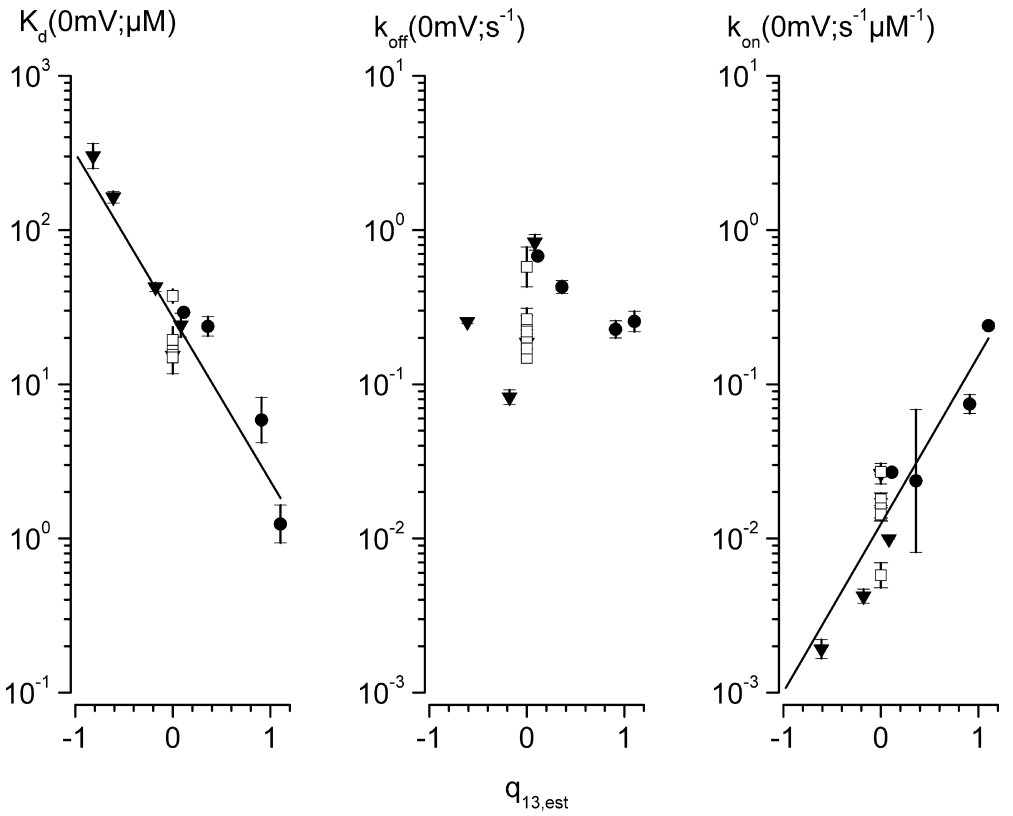

FIGURE 8. Correlation between binding kinetics and the bound-state charge of residue 13. K_d and k_{on} show a clear correlation with estimated residue 13 charge ($q_{13,est}$), as determined from the titrated fraction of $F_{res}(0)$ from Fig. 3 B. The lack of correlation between k_{off} and $q_{13,est}$ suggests that bound times are limited by short range chemical interactions, rather than the pH-dependent charge changes in residue 13. For R13A, $q_{13,est}$ is set to 0.

the titration site is essentially identical to our own estimate in the vicinity of bound toxin residue 13.

If all of these different analyses were accurately sampling precisely the same space, this would leave unanswered the question of why the presence of a bound conotoxin should not appear to substantially increase the local potential. However, the different assays used in these studies almost inevitably sample a somewhat different local potential on an atomic scale. Consequently, we are not convinced that there is a fundamental conflict reflected by the different numerical results.

Furthermore, in studies by Karlin and collaborators, the reaction rates of charged methanesulfonate reagents with selectively inserted cysteine residues were used to map the potential in the nicotinic acetylcholine receptor channel (Pascual and Karlin, 1998; Wilson et al., 2000). Their estimates of local potential within the pore ranged as negative as −230 mV, with extremely steep potential gradients ($\Delta\psi > 100$ mV over ~10 Å). This not only makes our own estimates of local potential at a defined location in the Na channel vestibule look relatively modest, but also emphasizes the point that potential estimates made with atomic scale probes can be expected to be exquisitely sensitive to their position on a scale of Å.

In our own study, the shifts in residue 13 pK from solution to the bound-state vestibule (pK_{Fres} - pK_{NMR}) were 3.15 and 2.15 for glutamate and histidine respectively. This difference is intriguing, and may result in part from the fact that the titrations occur over different pH ranges, and hence in the context of different charge arrays, for the two derivatives. Any conformational differences between these two situations would further complicate the interpretation of the difference in pK shifts for glutamate and histidine. As a convenient working hypothesis, and to give some quantitative sense for the energetic implications of our results, we interpret the shifts in purely electrostatic terms. We see this as no less useful—and no more rigorous—than the interpretation of voltage dependence of gating or channel block in terms of effective gating charge or electrical distance to a blocking site. We do, however, consider the estimate of a local potential as a useful interpretive device.

pH Dependence of Toxin Binding

The estimate of residue 13 pK in R13E and R13H from binding kinetics could, in principle, have been affected by proton block of the sodium channel. For example, at low pH, TTX shows reduced binding affinity whereas at high pH the toxin affinity saturates (Ulbricht and Wagner, 1975; Huang et al., 1979; Ulbricht et al., 1986). The reduction in TTX affinity appears to involve a site lying ~40% through the membrane voltage drop (Ulbricht et al., 1986), with pK identical to the channel. So, the pH dependence of this small guanidinium toxin seems to reside not in its own titration, but rather

in the competition with protons for a common site. It is less likely, however, that the pH dependence of the R13E and R13H μCTX mutants can be solely ascribed to this mechanism. First, although μCTX has some functional similarity to TTX (i.e., both are site 1 toxins; Catterall, 1992), it is unlikely to penetrate as deeply as do protons. Second, μCTX has more extensive interactions with the channel vestibule than TTX. In particular, although the guanidinium toxins appear to share the need for a charged outer ring on the channel (Noda et al., 1989; Terlau et al., 1991; Kontis and Goldin, 1993; Lipkind and Fozzard, 1994; Stephan et al., 1994), TTX binding requires a phenylalanine or tyrosine adjacent to the selectivity filter residue in domain I (Backx et al., 1992; Satin et al., 1992). In contrast, μCTX affinity is not particularly sensitive to point mutations in the DEKA filter (Dudley et al., 1995; Chang et al., 1998), but it is affected by mutations of residues in the outer charged ring and even outside the pore loops (Li et al., 1997; Chahine et al., 1998; Chang et al., 1998; Li et al., 2000, 2003). These differences between the actions of μCTX and TTX suggest that the former does not compete in a simple manner with proton block. Finally, there is a clear correlation between residue 13 charge in the bound state, and toxin equilibrium dissociation constant and association rate constant (Fig. 8). Overall, the data suggest that the pH dependent changes in the kinetics of μCTX result from titration of side chains of both the toxin and/or channel, with a major influence from toxin residue 13.

Residue 13 is a crucial determinant of μCTX block of sodium channels (Lancelin et al., 1991; Sato et al., 1991; Becker et al., 1992). Arguably, the need to use μM concentrations of a toxin might raise questions about its specificity. All residue 13 derivatives require relatively high concentrations (from submicromolar to submillimolar) for substantial binding. However, there is evidence that the block is specific. First, the discrete events that we observe as partial block of the unitary current exhibit a single conductance, suggesting that these toxin derivatives bind to a specific site on the channel. Second, the concentration of applied toxin does not affect the residual current; instead, it is consistent with a single toxin binding site (unpublished data). Third, the fractional residual current is pH dependent only for toxins with a titratable residue 13, and the titration is consistent with a single proton binding site. The fact that a residue 13–dependent titration is seen with residues so chemically different as glutamate and histidine is consistent with maintenance of a fixed toxin orientation in the pore despite the different substitutions. Collectively, these points indicate that the μCTX residue 13 derivatives bind with a one-to-one stoichiometry to the sodium channel, analogous to the wild-type toxin.

The Permeation Pathway

Ion permeation through highly selective cation ion channels has long been thought to involve the independent (Hodgkin and Huxley, 1952) or single-file (Hodgkin and Keynes, 1955) motion of ions through discrete pathways, dependent on the channel type and the conditions. In the case of voltage-dependent potassium channels, this pathway involves as many as four discrete electronegative ion binding sites, with high flux achieved by a billiard-ball mechanism (Morals-Cabral et al., 2001; Zhou et al., 2001; Miller, 2001). In voltage-dependent calcium channels, a similar mechanism has been proposed with two sites (Tsien et al., 1987; Ellinor et al., 1995). In voltage-dependent sodium channels, probably two sites are needed to account for the available data (French et al., 1994), but significant double occupancy appears likely only at very high sodium concentrations (Ravindran et al., 1992), despite difficulties in the interpretation of complex datasets (Naranjo and Latorre, 1993). If the acidic residues of the selectivity filter (aspartate and glutamate in domains I and II, respectively) contribute to one of these sites, then perhaps the outer ring of charged residues (lying three residues away) contributes to the second one. In support of this, neutralization of one of the outer ring charges (E758C) exhibits a reduced conductance (Chiamvimonvat et al., 1996).

Recent models indicate that μCTX interacts intimately with the outer charged ring of the sodium channel, particularly E758, and that even the native toxin may not completely sterically occlude the pore (Hui et al., 2002). Interestingly, the partial block that we see with R13A is similar to the reduced conductance of E758C channels, providing further support for the intimate interaction between R13 and E758. Consistent with the role of E758 in conduction, and from toxin-channel coupling studies (Chang et al., 1998), binding appears to be displaced off-center from the pore axis so that the toxin does not completely plug the pore, in contrast to the case for charybdotoxin and agitoxin block of potassium channels (Miller, 1995; MacKinnon et al., 1998). Taken together, μCTX R13X derivatives appear to block one portion of the permeation pathway, but they leave space for ions to traverse. The more complete block by the native μCTX may result from strategic charge placement, rather than complete steric occlusion. In contrast, TTX and STX block at the selectivity filter (Penzotti et al., 1998), leaving no current (French et al., 1984; Moczydlowski et al., 1984a,b). Perhaps there are multiple roads entering the pore, approaching one selectivity filter. This possibility is raised by a low resolution three-dimensional structure (Catterall, 2001; Sato et al., 2001). It is difficult, however, to see how a molecule of the size of μCTX could essentially completely block single channel current in the

4-port structure of Sato et al. (2001). A complete understanding doubtless will require further functional studies and a high resolution structure.

We are grateful to Dr. Denis McMaster for meticulous peptide synthesis and purification, and to Dr. Hans Vogel and the University of Calgary Bio-NMR Centre for assistance and use of the facilities. We thank Drs. R. MacKinnon and K. Beam for valuable suggestions and discussions during the course of the work. Drs. Harry Fozzard and Gregory Lipkind provided much appreciated, perceptive, and thought-provoking comments on the manuscript.

This work was supported by operating funds from the Canadian Institutes of Health Research. Maintenance and operation of the Bio-NMR Centre is supported by the Canadian Institutes of Health Research and the University of Calgary. R.J. French received salary support as an MRC Distinguished Scientist and a Heritage Medical Scientist of the Alberta Heritage Foundation for Medical Research.

Lawrence G. Palmer served as editor.

Submitted: 2 April 2003
Revised: 21 May 2003
Accepted: 22 May 2003

REFERENCES

Backx, P.H., D.T. Yue, J.H. Lawrence, E. Marban, and G.F. Tomaselli. 1992. Molecular localization of an ion-binding site within the pore of mammalian sodium channels. *Science.* 257:248–251.

Becker, S., E. Prusak-Sochaczewski, G. Zamponi, A.G. Beck-Sickinger, R.D. Gordon, and R.J. French. 1992. Action of derivatives of μ-conotoxin GIIIA on sodium channels. Single amino acid substitutions in the toxin separately affect association and dissociation rates. *Biochemistry.* 31:8229–8238.

Begenisich, T., and M. Dankó. 1983. Hydrogen ion block of the sodium pore in squid giant axons. *J. Gen. Physiol.* 82:599–618.

Benitah, J., J.R. Balser, E. Marban, and G.F. Tomaselli. 1997. Proton inhibition of sodium channels: mechanism of gating shifts and reduced conductance. *J. Membr. Biol.* 155:121–131.

Catterall, W.A. 1992. Cellular and molecular biology of voltage-gated sodium channels. *Physiol. Rev.* 72:S15–S48.

Catterall, W.A. 2001. A 3D view of sodium channels. *Nature.* 409: 988–991.

Chahine, M., J. Sirois, P. Marcotte, L. Chen, and R.G. Kallen. 1998. Extrapore residues of the S5-S6 loop of domain 2 of the voltage-gated skeletal muscle sodium channel (rSkM1) contribute to the mu-conotoxin GIIIA binding site. *Biophys. J.* 75:236–246.

Chang, N.S., R.J. French, G.M. Lipkind, H.A. Fozzard, and S. Dudley, Jr. 1998. Predominant interactions between μ-conotoxin Arg-13 and the skeletal muscle Na^+ channel localized by mutant cycle analysis. *Biochemistry.* 37:4407–4419.

Chen, X.-H., I. Bezprozvanny, and R.W. Tsien. 1996. Molecular basis of proton block of T-type Ca^{2+} channels. *J. Gen. Physiol.* 108: 363–374.

Chiamvimonvat, N., M.T. Pérez-García, G.F. Tomaselli, and E. Marban. 1996. Control of ion flux and selectivity by negatively charged residues in the outer mouth of rat sodium channels. *J. Physiol.* 491:51–59.

Colquhoun, D., and F.J. Sigworth. 1995. Fitting and statistical analysis of single-channel records. *In* Single-Channel Recording. B. Sakmann and E. Neher, editors. Plenum Press, New York. 483–587.

Creighton, T.E. 1993. Proteins: Structures and Molecular Properties. W.H. Freeman and Company, New York.

Cruz, L.J., W.R. Gray, B.M. Olivera, R.D. Zeikus, L. Kerr, D. Yoshikami, and E. Moczydlowski. 1985. *Conus geographus* toxins that discriminate between neuronal and muscle sodium channels. *J. Biol. Chem.* 260:9280–9288.

Cruz, L.J., G. Kupryszewski, G.W. LeCheminant, W.R. Gray, B.M. Olivera, and J. Rivier. 1989. μ-Conotoxin GIIIA, a peptide ligand for muscle sodium channels: Chemical synthesis, radiolabeling, and receptor characterization. *Biochemistry.* 28:3437–3442.

Daumas, P., and O.S. Andersen. 1993. Proton block of rat brain sodium channels: evidence for two proton binding sites and multiple occupancy. *J. Gen. Physiol.* 101:27–43.

De Biasi, M., J.A. Drewe, G.E. Kirsch, and A.M. Brown. 1993. Histidine substitution identifies a surface position and confers Cs+ selectivity on a K+ pore. *Biophys. J.* 65:1235–1242.

Delisle, B.P., and J. Satin. 2000. pH modification of human T-type calcium channel gating. *Biophys. J.* 78:1895–1905.

Doyle, D.A., J.M. Cabral, R.A. Pfuetzner, A. Kuo, J.M. Gulbis, S.L. Cohen, B.T. Chait, and R. MacKinnon. 1998. The structure of the potassium channel: molecular basis of K^+ conduction and selectivity. *Science.* 280:69–77.

Dudley, S.C., Jr., H. Todt, G. Lipkind, and H.A. Fozzard. 1995. A μ-conotoxin-insensitive Na^+ channel mutant: possible localization of a binding site at the outer vestibule. *Biophys. J.* 69:1657–1665.

Ellinor, P.T., J. Yang, W.A. Sather, J.F. Zhang, and R.W. Tsien. 1995. Ca^{2+} channel selectivity at a single locus for high-affinity Ca^{2+} interactions. *Neuron.* 15:1121–1132.

Frankenhaeuser, B., and A.L. Hodgkin. 1957. The action of calcium on the electrical properties of squid axons. *J. Physiol.* 137: 218–244.

French, R.J., and S.C. Dudley, Jr. 1999. Pore-blocking toxins as probes of voltage-dependent channels. *Methods Enzymol.* 294:575–605.

French, R.J., J.F. Worley III, and B.K. Krueger. 1984. Voltage-dependent block by saxitoxin of voltage-dependent sodium channels incorporated into planar lipid bilayers. *Biophys. J.* 45:301–310.

French, R.J., J.F. Worley III, W.F. Wonderlin, A.S. Kularatna, and B.K. Krueger. 1994. Ion permeation, divalent ion block and chemical modifications of single sodium channels: description by single-occupancy, rate theory models. *J. Gen. Physiol.* 103:447–470.

French, R.J., J.F. Worley, III, M.B. Blaustein, W.O. Romine, Jr., K.K. Tam, and B.K. Krueger. 1986. Gating of batrachotoxin-activated sodiuim channels in lipid bilayers. *In* Ion Channel Reconstitution. C. Miller, editor. Plenum Publishing Corporation. 363–383.

Green, M.E. 2002. Water as a structural element in a channel: gating in the Kcsa channel, and implications for voltage-gated ion channels. *J. Biomol. Struct. Dyn.* 19:725–730.

Green, W.N., L.B. Weiss, and O.S. Andersen. 1987. Batrachotoxin-modified sodium channels in planar lipid bilayers. Ion permeation and block. *J. Gen. Physiol.* 89:841–872.

Guo, X., A. Uehara, A Ravindran, S.H. Bryant, S. Hall, E. Moczydlowski. 1987. Kinetic basis of the insensitivity to tetrodotoxin and saxitoxin in sodium channels of canine heart and denervated rat skeletal muscle. *Biochemistry.* 26:7546–7556.

Heginbotham, L., M. LeMasurier, L. Kolmakova-Partensky, and C. Miller. 1999. Single streptomyces lividans K(+) channels: functional asymmetries and sidedness of proton activation. *J. Gen. Physiol.* 114:551–560.

Heinemann, S.H., H. Terlau, W. Stühmer, K. Imoto, and S. Numa. 1992. Calcium channel characteristics conferred on the sodium channel by single mutations. *Nature.* 356:441–443.

Hille, B. 1968. Charges and potentials at the nerve surface: divalent ions and pH. *J. Gen. Physiol.* 51:221–236.

Hille, B. 1977a. Local anesthetics: hydrophilic and hydrophobic pathways for the drug-receptor reaction. *J. Gen. Physiol.* 69:497–

515.
Hille, B. 1977b. The pH-dependent rate of action of local anesthetics on the node of Ranvier. *J. Gen. Physiol.* 69:475–496.
Hille, B., A.M. Woodhull, and B.I. Shapiro. 1975. Negative surface charge near sodium channels of nerve: divalent ions, monovalent ions, and pH. *Philos. Trans. R. Soc. Lond. B. Biol. Sci.* 270:301–318.
Hodgkin, A.L., and A.F. Huxley. 1952. Currents carried by sodium and potassium ions through the membrane of the giant axon of Loligo. *J. Physiol.* 116:449–472.
Hodgkin, A.L., and R.D. Keynes. 1955. The potassium permeability of a giant nerve fibre. *J. Physiol.* 128:61–88.
Hoth, S., and R. Hedrich. 1999. Distinct molecular bases for pH sensitivity of the guard cell K+ channels KST1 and KAT1. *J. Biol. Chem.* 274:11599–11603.
Huang, L.-Y.M., W.A. Catterall, and G. Ehrenstein. 1979. Comparsion of ionic selectivity of batrachotoxin-activated channels with different tetrodotoxin dissociation constants. *J. Gen. Physiol.* 73: 839–854.
Hui, K., G. Lipkind, H.A. Fozzard, and R.J. French. 2002. Electrostatic and steric contributions to block of the skeletal muscle sodium channel by μ-conotoxin. *J. Gen. Physiol.* 119:45–54.
Hwang, T.-L., and A.J. Shaka. 1995. Water suppression that works. Excitation sculpting using arbitrary waveforms and pulsed field gradients. *J. Magn. Reson. A.* 112:275–279.
Kehl, S.J., C. Eduljee, D.C. Kwan, S. Zhang, and D. Fedida. 2002. Molecular determinants of the inhibition of human Kv1.5 potassium currents by external protons and Zn(2+). *J. Physiol.* 541:9–24.
Khan, A., L. Romantseva, A. Lam, G. Lipkind, and H.A. Fozzard. 2002. Role of outer ring carboxylates of the rat skeletal muscle sodium channel pore in proton block. *J. Physiol.* 543:71–84.
Khodorov, B.I. 1985. Batrachotoxin as a tool to study voltage-sensitive sodium channels of excitable membranes. *Prog. Biophys. Mol. Biol.* 45:57–148.
Kontis, K.J., and A.L. Goldin. 1993. Site-directed mutagenesis of the putative pore region of the rat IIA sodium channel. *Mol. Pharmacol.* 43:635–644.
Lancelin, J.-M., D. Kohda, S.-I. Tate, Y. Yanagawa, T. Abe, M. Satake, and F. Inagaki. 1991. Tertiary structure of conotoxin GIIIA in aqueous solution. *Biochemistry.* 30:6908–6916.
Li, R.A., I.L. Ennis, T. Xue, H.M. Nguyen, G.F. Tomaselli, A.L. Goldin, and E. Marban. 2003. Molecular basis of isoform-specific μ-conotoxin block of cardiac, skeletal muscle, and brain Na^+ channels. *J. Biol. Chem.* 278:8717–8724.
Li, R.A., R.G. Tsushima, R.G. Kallen, and P.H. Backx. 1997. Pore residues critical for μ-CTX binding to rat skeletal muscle Na^+ channels revealed by cysteine mutagenesis. *Biophys. J.* 73:1874–1884.
Li, R.A., P. Vélez, N. Chiamvimonvat, G.F. Tomaselli, and E. Marbán. 2000. Charged residues between the selectivity filter and S6 segments contribute to the permeation phenotype of the sodium channel. *J. Gen. Physiol.* 115:81–92.
Lipkind, G.M., and H.A. Fozzard. 1994. A structural model of the tetrodotoxin and saxitoxin binding site of the Na^+ channel. *Biophys. J.* 66:1–13.
Lopes, C.M., P.G. Gallagher, M.E. Buck, M.H. Butler, and S.A. Goldstein. 2000. Proton block and voltage gating are potassium-dependent in the cardiac leak channel Kcnk3. *J. Biol. Chem.* 275: 16969–16978.
Lopes, C.M., Y. Zilberter, and S.A. Goldstein. 2001. Block of Kcnk3 by protons. Evidence that the 2-P-domain potassium channel subunits function as homodimers. *J. Biol. Chem.* 276:24449–24452.
MacKinnon, R., S.L. Cohen, A. Kuo, A. Lee, and B.T. Chait. 1998. Structural conservation in prokaryotic and eukaryotic potassium channels. *Science.* 280:106–109.
McManus, O.B., A.L. Blatz, and K.L. Magleby. 1987. Sampling, log binning, fitting, and plotting durations of open and shut intervals from single channels and the effects of noise. *Pflugers Arch.* 410:530–553.
Miller, C. 1986. Reconstitution of Ion Channel Proteins. Plenum Press, New York. 577 pp.
Miller, C. 1995. The charybdotoxin family of K^+ channel-blocking peptides. *Neuron.* 15:5–10.
Miller, C. 2001. See potassium run. *Nature.* 414:23–24.
Moczydlowski, E. 1998. Chemical basis for alkali cation selectivity in potassium-channel proteins. *Chem. Biol.* 5:R291–R301.
Moczydlowski, E., S.S. Garber, and C. Miller. 1984a. Batrachotoxin-activated sodium channels in planar lipid bilayers: competition of tetrodotoxin block by Na^+. *J. Gen. Physiol.* 84:665–686.
Moczydlowski, E., S. Hall, S.S. Garber, G.R. Strichartz, and C. Miller. 1984b. Voltage-dependent blockade of muscle Na^+ channels by guanidinium toxins: Effect of toxin charge. *J. Gen. Physiol.* 84:687–704.
Moczydlowski, E., B.M. Olivera, W.R. Gray, and G.R. Strichartz. 1986. Discrimination of muscle and neuronal Na-channel subtypes by binding competition between [^{3}H]saxitoxin and μ-conotoxins. *Proc. Natl. Acad. Sci. USA.* 83:5321–5325.
Morals-Cabral, J.H., Y. Zhou, and R. MacKinnon. 2001. Energetic optimization of ion conduction rate by the K^+ selectivity filter. *Nature.* 414:37–42.
Naranjo, D., and R. Latorre. 1993. Ion conduction in substates of the batrachotoxin-modified Na^+ channel from toad skeletal muscle. *Biophys. J.* 64:1038–1050.
Noda, M., H. Suzuki, S. Numa, and W. Stuhmer. 1989. A single point mutation confers tetrodotoxin and saxitoxin insensitivity on the sodium channel II. *FEBS Lett.* 259:213–216.
Pascual, J.M., and A. Karlin. 1998. State-dependent accessibility and electrostatic potential in the channel of the acetylcholine receptor. Inferences from rates of reaction of thiosulfonates with substituted cysteines in the M2 segment of the a subunit. *J. Gen. Physiol.* 111:717–739.
Penzotti, J.L., H.A. Fozzard, G.M. Lipkind, and S.C. Dudley, Jr. 1998. Differences in saxitoxin and tetrodotoxin binding revealed by mutagenesis of the Na^+ channel outer vestibule. *Biophys. J.* 75: 2647–2657.
Pietrobon, D., B. Prod'hom, and P. Hess. 1989. Interactions of protons with single open L-type calcium channels. pH dependence of proton-induced current fluctuations with Cs^+, K^+, and Na^+ as permeant ions. *J. Gen. Physiol.* 94:1–21.
Prod'hom, B., D. Pietrobon, and P. Hess. 1989. Interactions of protons with single open L-type calcium channels. Location of protonation site and dependence of proton- induced current fluctuations on concentration and species of permeant ion. *J. Gen. Physiol.* 94:23–42.
Ravindran, A., H. Kwiecinski, O. Alvarez, G. Eisenman, and E. Moczydlowski. 1992. Modeling ion permeation through batrachotoxin-modified Na^+ channels from rat skeletal muscle with a multi-ion pore. *Biophys. J.* 61:494–508.
Root, M.J., and R. MacKinnon. 1994. Two identical noninteracting sites in an ion channel revealed by proton transfer. *Science.* 265: 1852–1856.
Satin, J., J.W. Kyle, M. Chen, P. Bell, L.L. Cribbs, H.A. Fozzard, and R.B. Rogart. 1992. A mutant of TTX-resistant cardiac sodium channels with TTX-sensitive properties. *Science.* 256:1202–1205.
Sato, C., Y. Ueno, K. Asai, K. Takahashi, M. Sato, A. Engel, and Y. Fujiyoshi. 2001. The voltage-sensitive sodium channel is a bell-shaped molecule with several cavities. *Nature.* 409:1047–1051.
Sato, K., Y. Ishida, K. Wakamatsu, R. Kato, H. Honda, H. Nakamura,

M. Ohya, D. Kohda, F. Inagaki, J.-M. Lancelin, and Y. Ohizumi. 1991. Active site of μ-conotoxin GIIIA, a peptide blocker of muscle sodium channels. *J. Biol. Chem.* 266:16989–16991.

Schwarz, W., P.T. Palade, and B. Hille. 1977. Local anesthetics: Effect of pH on use-dependent block of sodium channels in frog muscle. *Biophys. J.* 20:343–368.

Stephan, M.M., J.F. Potts, and W.S. Agnew. 1994. The microI skeletal muscle sodium channel: mutation E403Q eliminates sensitivity to tetrodotoxin but not to mu-conotoxins GIIIA and GIIIB. *J. Membr. Biol.* 137:1–8.

Stocker, M., and C. Miller. 1994. Electrostatic distance geometry in a K^+ channel vestibule. *Proc. Natl. Acad. Sci. USA.* 91:9509–9513.

Sun, Y.-M., I. Favre, L. Schild, and E. Moczydlowski. 1997. On the structural basis for size-selective permeation of organic cations through the voltage-gated sodium channel. Effect of alanine mutations at the DEKA locus on selectivity, inhibition by Ca^{2+} and H^+, and molecular sieving. *J. Gen. Physiol.* 110:693–715.

Terlau, H., S.H. Heinemann, W. Stuhmer, M. Pusch, F. Conti, K. Imoto, and S. Numa. 1991. Mapping the site of block by tetrodotoxin and saxitoxin of sodium channel II. *FEBS Lett.* 293:93–96.

Tsien, R.W., P. Hess, E.W. McCleskey, and R.L. Rosenberg. 1987. Calcium channels: mechanisms of selectivity, permeation, and block. *Annu. Rev. Biophys. Biophys. Chem.* 16:265–290.

Uehara, A., and J.R. Hume. 1985. Interactions of organic calcium channel antagonists with calcium channels in single frog atrial cells. *J. Gen. Physiol.* 85:621–647.

Ulbricht, W., and H.-H. Wagner. 1975. The reaction between tetrodotoxin and membrane sites at the node of Ranvier: its kinetics and dependence on pH. *Philos. Trans. R. Soc. Lond. B Biol. Sci.* 270:353–363.

Ulbricht, W., H.H. Wagner, and J. Schmidtmayer. 1986. Kinetics of TTX-STX block of sodium channels. *Ann. NY Acad. Sci.* 479:68–83.

Vivaudou, M., and C. Forestier. 1995. Modification by protons of frog skeletal muscle KATP channels: effects on ion conduction and nucleotide inhibition. *J. Physiol.* 486:629–645.

Wakamatsu, K., D. Kohda, H. Hatanaka, J.-M. Lancelin, Y. Ishida, M. Oya, H. Nakamura, F. Inagaki, and K. Sato. 1992. Structure-activity relationships of μ-conotoxin GIIIA: structure determination of active and inactive sodium channel blocker peptides by NMR and simulated annealing calculations. *Biochemistry.* 31: 12577–12584.

Wilson, G.G., J.M. Pascual, N. Brooijmans, D. Murray, and A. Karlin. 2000. The intrinsic electrostatic potential and the intermediate ring of charge in the acetylcholine receptor channel. *J. Gen. Physiol.* 115:93–106.

Wonderlin, W.F., R.J. French, and N.J. Arispe. 1990. Recording and analysis of currents from single ion channels. *In* Neuromethods. Vol. 14. AA. Boulton, G.B. Baker, and C.H. Vanderwolf, editors. Humana Press, NJ. 35–142.

Woodhull, A.M. 1973. Ionic blockage of sodium channels in nerve. *J. Gen. Physiol.* 61:687–708.

Zamponi, G.W., D.D. Doyle, and R.J. French. 1993a. Fast lidocaine block of cardiac and skeletal muscle sodium channels: One site with two routes of access. *Biophys. J.* 65:80–90.

Zamponi, G.W., D.D. Doyle, and R.J. French. 1993b. State-dependent block underlies the tissue specificity of lidocaine action on batrachotoxin-activated cardiac sodium channels. *Biophys. J.* 65: 91–100.

Zhang, J.-F., and S.A. Siegelbaum. 1991. Effects of external protons on single cardiac sodium channels from guinea pig ventricular myocytes. *J. Gen. Physiol.* 98:1065–1083.

Zhou, Y., J.H. Morals-Cabral, A. Kaufman, and R. MacKinnon. 2001. Chemistry of ion coordination and hydration revealed by a K^+ channel-Fab complex at 2.0 Å resolution. *Nature.* 414:43–48.